



## Cytotoxicity inhibition of catechol's type molecules by grafting on TiO<sub>2</sub> and Fe<sub>2</sub>O<sub>3</sub> nanoparticles surface

Elena Badetti<sup>a,\*</sup>, Andrea Brunelli<sup>a</sup>, Eleonora Faraggiana<sup>a</sup>, Judit Kalman<sup>b</sup>, Cinzia Bettiol<sup>a</sup>, Francesca Caterina Izzo<sup>a</sup>, José Maria Navas<sup>b</sup>, Antonio Marcomini<sup>a</sup>

<sup>a</sup> DAIS - Department of Environmental Sciences, Informatics and Statistics, University Ca' Foscari of Venice, Via Torino 155, 30170 Venice Mestre, Italy

<sup>b</sup> INIA - Instituto Nacional de Investigación y Tecnología Agraria y Alimentaria, Crta. de la Coruña, km 7, 5, 28040 Madrid, Spain

### ARTICLE INFO

#### Keywords:

Interaction nanoparticles pollutants  
Modified nanoparticles  
Increase nanoparticles' coverage  
Catechols  
Cytotoxicity  
Fish cell lines

### ABSTRACT

The potential toxicity deriving from the interaction between chemicals and manufactured nanoparticles (NPs) represents an emerging threat to the environment and human health. Several studies have focused on the risks and (eco)toxicity of manufactured NPs as a consequence of their extensive use in recent years, however, there is still a limited understanding of the combined effects caused by manufactured NPs in the presence of other environmental contaminants. This is particularly relevant to aquatic environments, where many types of pollutants are inevitably released and can be involved in many kinds of reactions. In this context, the interaction between catecholate type ligands and two different nanomaterials, namely TiO<sub>2</sub> and Fe<sub>2</sub>O<sub>3</sub> NPs, was investigated by performing cytotoxicity assays with the topminnow fish hepatoma cell line (PLHC-1) using: i) the original organic molecules, ii) pristine NPs alone, and iii) modified NPs obtained by grafting the ligands on the NPs surface. Cytotoxic effects were explored at three different levels, specifically on cellular metabolism, membrane integrity and lysosomal activity. The outcomes from these assays showed cytotoxicity only for the free catechol type ligands, while in general no significant decrease in cell viability was observed for pristine NPs, as well as for the modified NPs, regardless the initial cytotoxicity level of the organic ligands. These results suggest that the binding of catechols on the NPs' surface inhibited their cytotoxicity, indicating that TiO<sub>2</sub> and Fe<sub>2</sub>O<sub>3</sub> NPs may act as sorbents of these contaminants, thus reducing their possible detrimental effects.

### 1. Introduction

Catechol (1,2-dihydroxybenzene) and catechol derivatives are organic compounds that can occur naturally in trace amounts, for instance as by-products from the breakdown of lignin by microorganisms, metabolites produced in the degradation process of chemicals by humans and mammals, as well as food constituents (e.g., caffeic acid, tea catechins, phenolic acids in legume tissues) (Schweigert et al., 2001). Catechol is also produced synthetically from phenols and it is widely used in the manufacturing process of pesticides, pharmaceuticals, dyes, rubber, plastic, and photographic products (Fiege et al., 2000). Due to their broad range of applications and low biodegradability, catecholate compounds can be found from concentrations of around 15 µg·L<sup>-1</sup> in river water (Zhao et al., 2007), up to concentrations of around 2 g·L<sup>-1</sup> in wastewaters from coal carbonization and gasification processes (Subramanyam and Mishra, 2008). Several studies have already reported the

toxicity of catechols to bacterial species, aquatic organisms and mammals, as well as their cytotoxic and genotoxic properties (Barreto et al., 2009; Schweigert et al., 2001). Given the high reactivity of catechols in the presence of heavy metals, oxidising agents, and different types of biomolecules, potential deleterious effects caused by the interaction between catecholate compounds and other contaminants should also be further investigated. Among emerging contaminants, manufactured nanoparticles (NPs) can represent a good candidate for deeply studying these interactions, due to their widespread production and use, which has raised concerns about the potential hazard posed to human health and the environment by these materials. In particular, the nanometric size of NPs leads to a high number of atoms and crystal lattice defects on their surface, which greatly enhances their surface reactivity and facilitates bio-physicochemical interactions at the bio-nano interface (Nel et al., 2013). This characteristic feature of NPs provides from one side the possibility to obtain novel functional nanomaterials for many

\* Corresponding author at: Department of Environmental Sciences, Informatics and Statistics, University Ca' Foscari of Venice, Via Torino 155, 30170 Venice Mestre, Italy.

E-mail address: [elena.badetti@unive.it](mailto:elena.badetti@unive.it) (E. Badetti).

<https://doi.org/10.1016/j.aquatox.2022.106291>

Received 18 March 2022; Received in revised form 3 August 2022; Accepted 5 September 2022

Available online 7 September 2022

0166-445X/© 2022 Elsevier B.V. All rights reserved.

applications, while on the other side it promotes the interaction with environmental components and biological systems, potentially leading to unwanted chemical/biological/toxicological reactivity. Possible mechanisms of toxic action of NPs include direct damage to biological membrane functioning, interaction with subcellular organelles such as lysosomes and mitochondria, physical interference caused by nano-composites with similar size and shape to those of the key cellular components, DNA impairment, protein inactivation, and generation of reactive oxygen species (ROS) (Shang et al., 2014).

In this paper, the interaction between four catechol type molecules bearing different functional groups (namely catechol, 3,4-dihydroxybenzaldehyde, 3,4-dihydroxybenzoic acid, dopamine hydrochloride) and two manufactured nanoparticles ( $\text{TiO}_2$  NPs and  $\text{Fe}_2\text{O}_3$  NPs) was investigated. To this purpose, modified NPs have been prepared by grafting these ligands on the nanoparticle surface, and their cytotoxicity was assessed by *in vitro* assays.

$\text{TiO}_2$  NPs and  $\text{Fe}_2\text{O}_3$  NPs have been selected because they are among the most-produced NPs in Europe (Ali et al., 2016; Sun et al., 2014; Piccinno et al., 2012) and they can be released into air, water, and soil during their entire life cycle, presenting sometimes adverse effects for human health and the environment (Slomberg et al., 2019). Catecholate type ligands have the right geometry to become covalently grafted onto both  $\text{TiO}_2$  and  $\text{Fe}_2\text{O}_3$  NPs' surfaces, by exploiting the atoms and crystal lattice defects present on the NPs' surfaces. The grafting has already been described to occur through bidentate binding involving the hydroxyl (-OH) groups, as well as the carboxyl (-COOH) group, if present (Basti et al., 2010; Brunelli et al., 2018; Korpany et al., 2017; Savić et al., 2014). In order to better understand such interactions, salicylic acid (SAL) and polyethylene glycol (PEG) were also tested: SAL presents a similar structure to catechol but with a -COOH group instead of an -OH group, while PEG has two -OH groups separated by a long alkyl linear chain, resulting in a more flexible structure than catechol.

The toxicity of the modified NPs was then evaluated with the aim to investigate their potential hazard as they might occur in aquatic environments. *In vitro* cytotoxicity tests using the topminnow fish (*Poeciliopsis lucida*) hepatoma cell line (PLHC-1) were performed to assess the effects on cell viability of both pristine and surface-modified NPs, as well as of the abovementioned organic ligands. The three cytotoxicity assays performed, which use the three indicator dyes AlamarBlue (AB), CFDA-AM, and Neutral Red (NR), provide information on the effects on cellular metabolism, membrane integrity and lysosomal activity, respectively, allowing thus to explore different cytotoxicity mechanisms and to identify the cellular processes affected by a potential toxicant. When dose-response curves show a similar decline in cell viability for the three indicator dyes, this normally indicates general membrane damage, including both the plasma membrane, as well as organelle membranes and/or functions. In some cases, only cellular metabolism or lysosomal functioning can be directly impacted after exposure to toxic compounds, while little or no impairment of plasma membrane integrity (measured with CFDA-AM assay) is observed (Dayeh et al., 2013).

Exploring the mechanisms of toxicity at cellular level through multiple *in vitro* assays can facilitate the screening of composite nanomaterials by reducing animal testing (Bermejo-Nogales et al., 2017) and can contribute to improve the understanding of the interactions occurring at the bio-nano interface (Alkilany et al., 2013; Lynch et al., 2014).

## 2. Materials and methods

### 2.1. Chemicals and reagents

The inorganic Aeroxide® P25 titanium dioxide ( $\text{TiO}_2$ ) nanopowder was purchased from Evonik Degussa (Germany). It is a mixture of approx. 80% anatase and 20% rutile, with 99.5% purity and a nominal average particle size of  $21 \pm 5$  nm. The inorganic iron oxide hematite ( $\text{Fe}_2\text{O}_3$ ) nanopowder was purchased from BASF (Germany) with an average particles size of 40 nm and purity  $\geq 98\%$ .

Catechol (CAT), 3,4-dihydroxybenzaldehyde (CHO), 3,4-dihydroxybenzoic acid (COOH), dopamine hydrochloride (DOP), salicylic acid (SAL), polyethylene glycol (PEG, Mw 100000), and all the other chemicals were of the highest purity available and were used without further purification (Sigma Aldrich, St. Louis, MI, USA). Ethanol was purchased from Romil (Ltd, Cambridge, UK) and ultrapure water with a resistivity of  $18.2 \text{ M}\Omega\text{cm}$  was obtained with MilliQ® system (Millipore).

For the cytotoxicity assays, all chemicals were purchased from Sigma Aldrich (Madrid, Spain) unless otherwise stated. Eagle's Minimum Essential Medium (EMEM) with non-essential aminoacids, (NEAA) and Na Pyruvate without L-Glutamine, Penicillin/Streptomycin (P/S, 10,000 units penicillin and streptomycin per mL), L-Glutamine solution (200 mM), and 100x NEAA were obtained from Lonza (Barcelona, Spain). Serum-free/phenol red-free MEM was purchased from PAN Biotech (Aidenbach, Germany). AlamarBlue (AB) reagent and 5-Carboxyfluorescein diacetate-acetoxymethyl ester (CFDA-AM) were acquired from Life Technologies (Madrid, Spain). Bovine serum albumin (BSA) was obtained from Merck (Darmstadt, Germany).

### 2.2. Synthesis of modified nanoparticles

#### 2.2.1. Grafting of organic ligands on $\text{TiO}_2$ and $\text{Fe}_2\text{O}_3$ NPs' surface

In order to investigate the cytotoxicity of the NPs-organic ligand compounds, both  $\text{TiO}_2$  and  $\text{Fe}_2\text{O}_3$  NPs were modified by grafting the selected organic ligands on the NPs' surface. According to the procedure already reported by some of us for  $\text{TiO}_2$  NPs (Brunelli et al., 2018), 200 mg of NPs were dispersed in 100 mL of ethanol ( $2 \text{ g}\cdot\text{L}^{-1}$ ) by sonication with an ultrasonic probe (UP-200S Hielscher Ultrasonics GmbH, Germany) in an ice bath, delivering a power of 200 W for 15 min using a pulsed 80% mode. The four catecholate type ligands (4 mM), SAL (4 mM) and PEG (0.4 mM) were dissolved in 25 mL of ethanol and mixed with 100 mL of each NPs dispersion. The 12 dispersions obtained were sonicated in an ice bath by an ultrasonic probe over 1 h and then stirred overnight at room temperature. Afterwards, each suspension was centrifuged until the NPs settled completely. The supernatant was removed, and the particles were washed three times by adding 10 mL of EtOH to remove the possible excess of unlinked ligand, followed by ultra-sonication and finally by centrifugation of the new suspension until the complete settling of the NPs. After the last washing step, the NPs were air dried leading to the corresponding modified materials as powders.

#### 2.2.2. Different procedures to increase the NPs' surface coverage

The number of organic molecules grafted on  $\text{TiO}_2$  NPs and  $\text{Fe}_2\text{O}_3$  NPs' surface was increased by choosing catechol as a model molecule and by applying the following experimental conditions:

1)  $\text{TiO}_2$ -CAT<sub>NPs-1</sub>: an ethanolic solution of catechol (30 mM) was added to an ethanolic suspension of  $\text{TiO}_2$  NPs ( $2 \text{ g}\cdot\text{L}^{-1}$ ), previously sonicated for 15 min with the ultrasonic probe in an ice bath (200 W in a pulsed 80% mode). The mixture obtained was probe sonicated at room temperature overnight. Then, the suspension was centrifuged until the NPs settled completely. The supernatant was discarded, and the particles were washed three times by adding 10 mL of EtOH to remove the possible excess of unlinked ligand, followed by ultra-sonication and finally by centrifugation of the new suspension until the complete settling of the NPs. After the last washing step, the NPs were dried leading to the corresponding modified materials as powders.

2)  $\text{TiO}_2$ -CAT<sub>NPs-2</sub>: an ethanolic solution of catechol (15 mM) was added to an ethanolic suspension of  $\text{TiO}_2$  NPs ( $2 \text{ g}\cdot\text{L}^{-1}$ ), previously sonicated for 15 min with the ultrasonic probe in an ice bath (200 W in a pulsed 80% mode). The obtained mixture was magnetically stirred at  $80^\circ\text{C}$  for 1 hour. After cooling, the suspension was centrifuged and the recovered solid was washed three times with EtOH as described above, until obtaining the modified material as a dry powder.

3)  $\text{TiO}_2$ -CAT<sub>NPs-3</sub>: 400 mg of  $\text{TiO}_2$  NPs were mixed with 300 mg of catechol in solid state and the mixture was heated for 2 min at  $105^\circ\text{C}$

(corresponding to the catechol melting point), and then magnetically stirred at 80°C for 1 h. After reaching room temperature, the recovered powder was dispersed in 10 mL of EtOH, and the suspension was bath sonicated for 15 min. Two more EtOH washing steps were performed, according to the procedure described above, until obtaining the modified material as a dry powder.

4) *TiO<sub>2</sub>-CAT\_NPs-4*: an ethanolic solution of catechol (15 mM) was added to an ethanolic suspension of TiO<sub>2</sub> NPs (2 g·L<sup>-1</sup>), which was previously sonicated for 15 min with the ultrasonic probe in an ice bath (200 W in a pulsed 80% mode). The mixture was magnetically stirred at 80°C until the solvent was completely evaporated (~1 hour). After cooling, the recovered solid was washed three times with EtOH as described above, until obtaining the modified material as a dry powder.

5) *TiO<sub>2</sub>-CAT\_NPs-5*: 400 mg of TiO<sub>2</sub> NPs were mixed with 500 mg of catechol, and the mixture was magnetically stirred at 130°C in the solid state for 1 h. After cooling, the mixture was washed three times with EtOH according to the procedure described above, until obtaining the modified material as a dry powder.

6) *Fe<sub>2</sub>O<sub>3</sub>-CAT\_NPs-6*: 400 mg of Fe<sub>2</sub>O<sub>3</sub> NPs were mixed with 500 mg of catechol in the solid state and the mixture was heated for 2 min at 105°C (corresponding to the catechol melting point), and then magnetically stirred at 80°C for 1 h. After reaching room temperature, the recovered powder was dispersed in 10 mL of EtOH, and the suspension was bath sonicated for 15 min. Then, the suspension was centrifuged, and the recovered solid was washed three times with EtOH and centrifuged as described above, until obtaining the modified material as a dry powder.

### 2.3. FTIR and TGA-DSC analysis

The dry powders' physicochemical characterization was performed by Fourier-Transform Infrared spectroscopy (FTIR), Thermo-Gravimetric Analysis (TGA) and Differential Scanning Calorimetry (DSC), as already described (Badetti et al., 2019; Brunelli et al., 2018). FTIR analysis was performed by a Thermo Nicolet Nexus 670 FTIR spectrophotometer equipped with a Smart Orbit Single Reflection Diamond ATR (Attenuated Total Reflection) accessory, from 4000 to 400 cm<sup>-1</sup> for 64 scans with 4 cm<sup>-1</sup> resolution. The data were elaborated with Omnic 8.0 and Origin 8.0 software.

TG and DSC analyses were simultaneously performed by means of a Netzsch 409/C apparatus. The temperature program used was set from 30 to 600°C, with a heating rate of 10°C min<sup>-1</sup>. For the analyses, the samples (~15 mg) were placed in a platinum/rhodium crucible; alumina was used for the internal calibration. Measurements were performed in oxidative atmosphere (air/N<sub>2</sub> 40/80 mL·min<sup>-1</sup>) mixture. Data were collected with STA Netzsch software and elaborated with Origin 8.0 software.

### 2.4. SEM analysis

The surface topography of pristine TiO<sub>2</sub> NPs, TiO<sub>2</sub>-CAT NPs obtained with the standard procedure (paragraph 2.2.) and TiO<sub>2</sub>-CAT\_NPs-3, was investigated by Scanning Electron Microscopy (SEM). The dry samples were suspended in EtOH (0.1-0.5 mg·mL<sup>-1</sup>) and briefly ultrasonicated. 3 µL of each suspension were deposited on a silicon wafer substrate and dried at 60°C for 18–24 h. SEM images were collected in high vacuum with a Zeiss Sigma VP Field Emission SEM, using an in-lens detector at 5.0 keV beam energy.

### 2.5. Nanoparticle dispersion protocol and DLS characterization

Nanoparticles were dispersed in cell culture medium (prepared as described in paragraph 2.6) using the NANOGENOTOX protocol (Jensen et al., 2011), commonly employed in several EU and international projects. Briefly, NPs were first pre-wetted in absolute ethanol (0.5 vol %) dispersed in 0.05% BSA in MilliQ® water at a concentration of 2.56

mg·mL<sup>-1</sup> and sonicated using a probe sonicator (6 mm horn) in continuous mode (Vibra-Cell™ VCX 130, Sonics, Newton, CT, USA) for 15 min. NP dispersions were diluted in the cell culture medium in the range of 2 - 256 µg·mL<sup>-1</sup>. The same procedure was applied to the free ligands used to functionalize the NPs. These exposure concentrations were selected according to those already reported in the literature for the same cell line (Bermejo-Nogales et al., 2017; Fernández-Cruz et al., 2013; Kalman et al., 2019).

Dynamic light scattering (DLS) was employed to determine the hydrodynamic particle size distribution of pristine and modified TiO<sub>2</sub> and Fe<sub>2</sub>O<sub>3</sub>-NPs suspended in the PLHC-1 cell culture medium. DLS measurements from suspensions obtained with the NANOGENOTOX dispersion protocol were carried out at 0 h and 72 h of incubation in the cell culture medium (according to the cytotoxicity test duration). Measurements were performed with the highest TiO<sub>2</sub> and Fe<sub>2</sub>O<sub>3</sub>-NP suspension concentrations (256 µg·mL<sup>-1</sup>). Size frequency distributions are reported in Table S1 and S2, according to three independent measurements, with each measurement consisting of four individual readings (Zetasizer Nano-ZS; Malvern Instruments Ltd., Malvern, UK). The width and average size of TiO<sub>2</sub> and Fe<sub>2</sub>O<sub>3</sub>-NP size distributions were estimated according to the polydispersity index (PDI) and Z-average (z-ave) values, respectively. Hydrodynamic sizes are reported according to intensity, volume, and number weighted distributions.

### 2.6. Cell culture and cytotoxicity measurements

PLHC-1 cells were obtained from the American Type Culture Collection (Manassas, VA, USA). Cells were maintained in EMEM (with NEAA, Na Pyruvate, and without L-Glutamine) supplemented with 1% L-glutamine, 1% P/S and 5% fetal bovine serum (FBS) at 30°C, 5% CO<sub>2</sub>. For cell treatments, medium was supplemented with 10% FBS in order to increase the stability of NP suspensions (Lammel and Navas, 2014). Cells were subcultured twice a week using trypsin EDTA (in phosphate buffered saline).

PLHC-1 cells were seeded in flat-bottomed 96-well plates (Greiner Bio-One GmbH, Germany) at a density of 5 × 10<sup>4</sup> cells mL<sup>-1</sup> (which, for a 100 µL volume, corresponds to 1.47 × 10<sup>4</sup> cells·cm<sup>-2</sup>). Following 24 h incubation, confluent cells were exposed to a concentration range of 0-256 µg mL<sup>-1</sup> of NPs (dilution factor 2) in a 100 µL volume for 72 h. This exposure time was selected to explore possible effects over a longer period, ensuring at the same time that cells were incubated with optimal nutrient supply in the exposure medium (no nutrient deficit was observed in the control cells) (Bermejo-Nogales et al., 2017). Control wells were treated with medium or medium plus BSA. Sodium Dodecyl Sulphate (SDS, 65.8-500 mM, dilution factor 1.5) served as a positive cytotoxicity control (Galbis-Martínez et al., 2018; Lammel et al., 2013). At least three independent experiments were carried out with a minimum of three replicates of each NP concentration in each plate.

Cell viability has been assessed by applying simultaneously on the same set of cells three different cytotoxicity assays (AB, CFDA-AM, and NR) according to Lammel et al. (2013). These assays provide information on alterations of cell metabolism, plasma membrane integrity and lysosomal functioning, respectively.

Following exposure to NPs, medium was removed, and cells were washed twice with PBS. Wells received 100 µl of 1.25% (v/v) AB and 4 µM CFDA-AM prepared in serum-free/phenol red-free MEM (containing 1% NEAA). Fluorescence was measured on a microplate reader (Tecan GENios, Männendorf, Switzerland) at a wavelength of 532/590 nm (excitation/emission) for AB, or at 485/535 nm for CFDA-AM after 30 min of incubation in the dark. Cells were washed with PBS and incubated with 100 µL of neutral red solution (33 µg mL<sup>-1</sup> in serum-free/phenol red-free MEM containing 1% NEAA) for 1 h in the dark. Following incubation, cells were rinsed with PBS and the retained dye was extracted with 100 µl of an acidified (1% glacial acetic acid) 50% ethanol/49% Milli-Q water solution (extraction solution). Thereafter, fluorescence was measured at 532/680 nm. The fluorescence values

were corrected for the cell-free control results and normalized against the medium control values. Potential interferences of NP dispersions with cytotoxicity assays were tested as previously described by Kalman et al. (2019). For that, cells were seeded and exposed to NPs exactly in the same way as described for the toxicity tests. After exposure, fluorescence was measured at the wavelengths corresponding to the cytotoxicity assays before and after washing cells twice with PBS. Thereafter, cells were incubated under exposure conditions with the conversion products of AB (resorufin) and CFDA-AM (carboxyfluorescein) and fluorescence determined at time 0 and 30 min at the corresponding wavelengths. After washing, neutral red was added, and fluorescence readouts measured at the corresponding times and wavelengths.

Cytotoxicity data were presented as mean ( $\pm$  standard error of the mean) of three independent experiments (for each experiment, each concentration was applied by triplicate in the culture plates). Statistical analyses were performed on Sigma Plot version 12 (Systat Software, Inc., Chicago, IL, USA). The program checks automatically for homogeneity of variance. The normality of the distribution was confirmed with Shapiro-Wilk test. One-way repeated measures analysis of variance (RMANOVA) was followed by post hoc Dunnett's test to compare the means of treatments (e.g., cytotoxicity assays) with respect to the control group.

### 3. Results and discussion

In order to investigate the interaction between catechol type ligands and both TiO<sub>2</sub> and Fe<sub>2</sub>O<sub>3</sub> NPs potentially occurring in the aquatic environment, the new nanomaterials formed according to the procedure described above were characterized from the physicochemical and ecotoxicological point of view, and the results obtained were compared with those obtained for both pristine NPs and free organic ligands as follows.

#### 3.1. Interaction between TiO<sub>2</sub> and Fe<sub>2</sub>O<sub>3</sub> NPs' surface and organic ligands

The chemisorption of the selected molecules to both NPs was investigated by means of FTIR-ATR and TG-DSC (Fe<sub>2</sub>O<sub>3</sub> NPs spectra are reported in Figures S0-S12, while TiO<sub>2</sub> NPs spectra are reported in Brunelli et al., 2018). In the case of FTIR-ATR analysis, the spectra of the modified NPs were compared with those of free organic ligands. As an example, the FTIR-ATR spectra of free CAT (Fig. 1a), of TiO<sub>2</sub>-CAT NPs (Fig. 1b) and of Fe<sub>2</sub>O<sub>3</sub>-CAT NPs (Fig. 1c) are displayed as a zoom-in image of the wavelength region between 1800-1000 cm<sup>-1</sup>.

According to the literature (Brunelli et al., 2018; Korpany et al., 2017; Savić et al., 2014; Yuen et al., 2012), the adsorption of catechol onto both NPs surfaces (Fig. 1b and c) led to a loss of the hyperfine structure of bending  $\delta$ (C-OH) vibration in the region below 1200 cm<sup>-1</sup>, the disappearance of the bands at 1360 and 1184 cm<sup>-1</sup> and the appearance of a very weak feature centred at 1329 cm<sup>-1</sup>. For both modified NPs, the band of stretching  $\nu$ (C-OH) vibrations were merged to a unique broad band at 1263 cm<sup>-1</sup>. These signals are related to the stretching and bending vibrations of the two phenolic groups that take part in the complex formation with both Ti and Fe surface atoms. In addition, the stretching bands in the region above 1400 cm<sup>-1</sup>, related to the aromatic ring, were also merged into a single band at 1485 cm<sup>-1</sup> because of the binding.

As far as the ATR-FTIR spectra of Fe<sub>2</sub>O<sub>3</sub> NPs modified with CHO, COOH, DOP, and SAL are concerned (Fig. S2-S5), they all showed two main adsorption bands at around 516 and 432 cm<sup>-1</sup>, due to the stretching of Fe-O bond, and less intense bands in the fingerprint region between 1000 and 1800 cm<sup>-1</sup>, related to the main groups of the organic ligands attached to the NPs' surface (e.g., phenol, carboxyl and amine groups). In the case of Fe<sub>2</sub>O<sub>3</sub>-PEG NPs (Fig. S6), a unique broad band at 1103 cm<sup>-1</sup> due to the ethylene glycol polymer was observed. Consistent with our previous work on TiO<sub>2</sub> NPs (Brunelli et al., 2018), the chemisorption of the selected ligands on the surface of Fe<sub>2</sub>O<sub>3</sub> NPs is likely to occur mainly through the binding between the phenolic OH groups and some of the Fe atoms on the NPs surface (Korpany et al., 2017; Yuen et al., 2012).

The TGA-DSC analyses of both pristine and modified NPs were carried out in the temperature range from 30 to 600°C (Figs. S7-S12, Brunelli et al., 2018). The amount of organic coverage as percent mass loss for each nano-based material was then estimated (Table 1). In general, TiO<sub>2</sub> NPs showed a higher amount of ligand grafted on their surface than Fe<sub>2</sub>O<sub>3</sub> NPs. This is likely related to a greater number of surface defects present on TiO<sub>2</sub> NPs' surface, due to their smaller size (~21 nm vs. ~40 nm). The chemisorption of the ligands was then confirmed by DSC analysis: the corresponding curves, obtained in oxidative atmosphere, showed exo-thermal processes associated with the decomposition of the attached organic fraction, occurring approximately between 200 and 400°C (Figs. S7-S12 and in Brunelli et al., 2018).

#### 3.2. Cytotoxicity assessment of the organic ligands, pristine and modified NPs

As described in the literature, there is a general difficulty of comparing results from different cytotoxicity studies with NPs due to

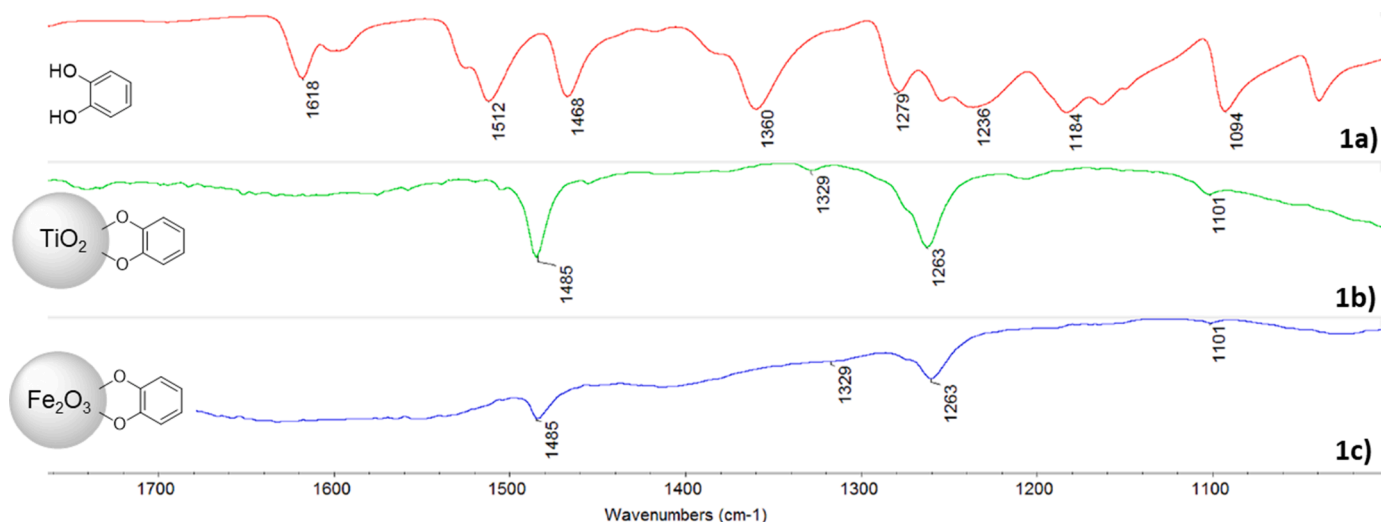


Fig. 1. ATR-FTIR spectra of (a) free catechol, (b) TiO<sub>2</sub>-CAT NPs, and (c) Fe<sub>2</sub>O<sub>3</sub> NPs-CAT in the region between 1800 and 1000 cm<sup>-1</sup>.

**Table 1**  
TGA results for surface modified TiO<sub>2</sub> NPs and Fe<sub>2</sub>O<sub>3</sub> NPs.

	Ligand	TiO <sub>2</sub> NPs- Ligand	Mass Loss (%)	Fe <sub>2</sub> O <sub>3</sub> NPs- Ligand	Mass Loss (%)
CAT		TiO <sub>2</sub> - CAT	3.9	Fe <sub>2</sub> O <sub>3</sub> - CAT	2.5
CHO		TiO <sub>2</sub> - CHO	6.3	Fe <sub>2</sub> O <sub>3</sub> - CHO	1.7
COOH		TiO <sub>2</sub> - COOH	4.3	Fe <sub>2</sub> O <sub>3</sub> - COOH	0.8
DOP		TiO <sub>2</sub> - DOP	3.8	Fe <sub>2</sub> O <sub>3</sub> - DOP	1.7
SAL		TiO <sub>2</sub> - SAL	7.0	Fe <sub>2</sub> O <sub>3</sub> - SAL	0.6
PEG		TiO <sub>2</sub> - PEG	8.9	Fe <sub>2</sub> O <sub>3</sub> - PEG	2.9

several factors (e.g., interaction between the NPs and the component of the dispersion medium, agglomeration and aggregation processes), which contribute to variable responses in the assays. Thus, a fundamental requirement for consistent toxicity testing is the evaluation of the possible interference of NPs with the components and processes involved, as well as a thorough physicochemical characterization of NPs during exposure (Lammel and Sturve, 2018).

In this context, prior to performing the cytotoxicity assays, experiments were carried out to determine i) aggregation of NPs in the culture medium used in the three assays, and ii) interferences that could potentially occur between the NPs and the biochemical methods employed to determine cytotoxicity. Thus, the hydrodynamic size distribution of both pristine and surface-modified TiO<sub>2</sub> and Fe<sub>2</sub>O<sub>3</sub> NPs in the PLHC-1 cell culture medium, at time 0 and after 72 h of incubation under the fish cell culture conditions, was investigated by DLS (Table S1 and S2). All the NPs showed a low level of agglomeration/aggregation, with a hydrodynamic particle diameter (according to intensity) of 200–260 nm for TiO<sub>2</sub> NPs and 240–290 nm for Fe<sub>2</sub>O<sub>3</sub> NPs, which remained stable over the exposure time of the assays (indicating homogenous dispersions). In addition, no interference was detected between the NPs or the organic molecules selected and the fluorescence wavelength signal of the three cytotoxicity assays used.

After these preliminary experiments, the cytotoxicity of pristine TiO<sub>2</sub>

and Fe<sub>2</sub>O<sub>3</sub> NPs was assessed. For all the assays no effect on PLHC-1 cell viability was observed up to the highest concentration used (256 µg·mL<sup>-1</sup>) (Fig. 2).

The absence of TiO<sub>2</sub> NPs cytotoxicity effects at the three levels explored within this study, i.e., cellular metabolism, membrane integrity and lysosomal activity, confirms the findings from a previous investigation conducted with various fish cell lines on different TiO<sub>2</sub> nano-materials (Bermejo-Nogales et al., 2017), as well as from other studies using the same or similar endpoints and comparable NPs concentrations (Lammel and Sturve, 2018; Reeves et al., 2008). Though the literature provides also evidence of cytotoxic effects of TiO<sub>2</sub> NPs in fish cell lines at significantly lower concentrations, it is worth to underline that these discrepancies may be ascribed to the fact that toxicity testing of nano-materials is quite challenging, due to their unique physico-chemical properties which lead to their peculiar behaviour (Lammel and Sturve, 2018). As thoroughly outlined by these authors, most studies do not provide sufficient information about the physicochemical properties, size distribution and colloidal stability of the investigated NPs, as well as on the possible interferences with the assays. They also underline the importance of the dispersion protocols used, which may explain the difficulty to compare the outcomes of different cytotoxicity studies, due to possible discrepancies between real and nominal concentrations (Lammel and Sturve, 2018).

As far as Fe<sub>2</sub>O<sub>3</sub> NPs are concerned, their toxicity has been evaluated mainly in relation to human health and biomedical applications, using mammalian cells, with different studies providing different and somehow contrasting findings, depending on the cell models and endpoints used. Our data are in accordance for example with those of Lai et al. (2015), who reported no cytotoxicity in lung epithelial cells, while Fe<sub>2</sub>O<sub>3</sub> NPs were shown to induce different cytotoxic effects in human lymphocytes (Rajiv et al. 2016). However, it is worth to underline that, though it is difficult to compare results from different cell lines, a consistency in the sensitivity of mammalian and fish cells has been shown in studies with both other types of NPs (Gaiser et al., 2009) and a number of different toxic chemicals (Castaño and Gómez-Lechón, 2005).

Differently from NPs, the four catechols tested in this study caused significant cytotoxicity (Fig. 3 and Table 2), while SAL and PEG had no significant effect on cell viability up to the highest tested concentration. In general, cytotoxicity followed the order CAT>CHO>COOH~DOP. Moreover, it can be seen that, except for DOP, the AB and NR assays yielded similar results, while the CFDA-AM assay exhibited a lower sensitivity, with significant effects only for CAT, DOP, and, to a lower extent, CHO.

The catecholate ligands affected cell viability at different concentration levels. Metabolic activity (AB assay) and lysosomal functionality (NR assay) were significantly inhibited already at 4 and 8 µg·mL<sup>-1</sup> by CAT and CHO, respectively, while COOH and DOP showed a lower

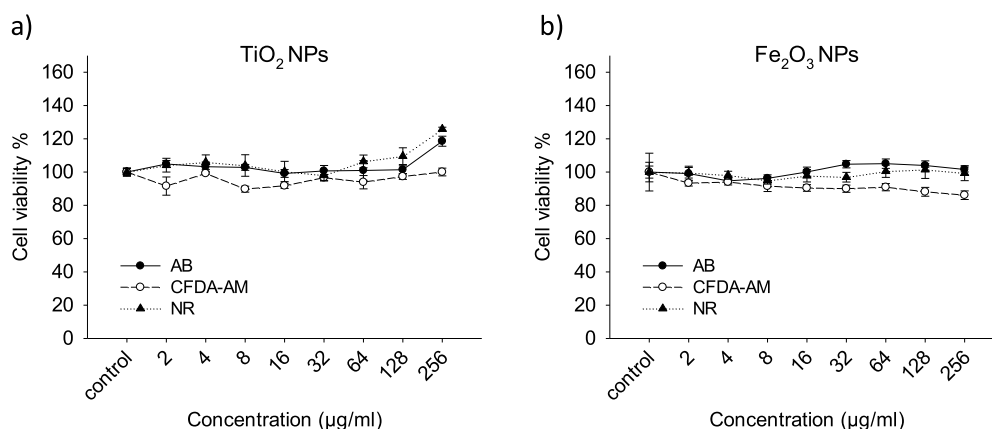


**Fig. 2.** Dose-response curves for pristine TiO<sub>2</sub> (a) and Fe<sub>2</sub>O<sub>3</sub> (b) NPs as measured by the three cytotoxicity assays (AB, CFDA-AM, and NR) in PLHC-1 cell line. Values represent the mean ± standard error of the mean (n=3).

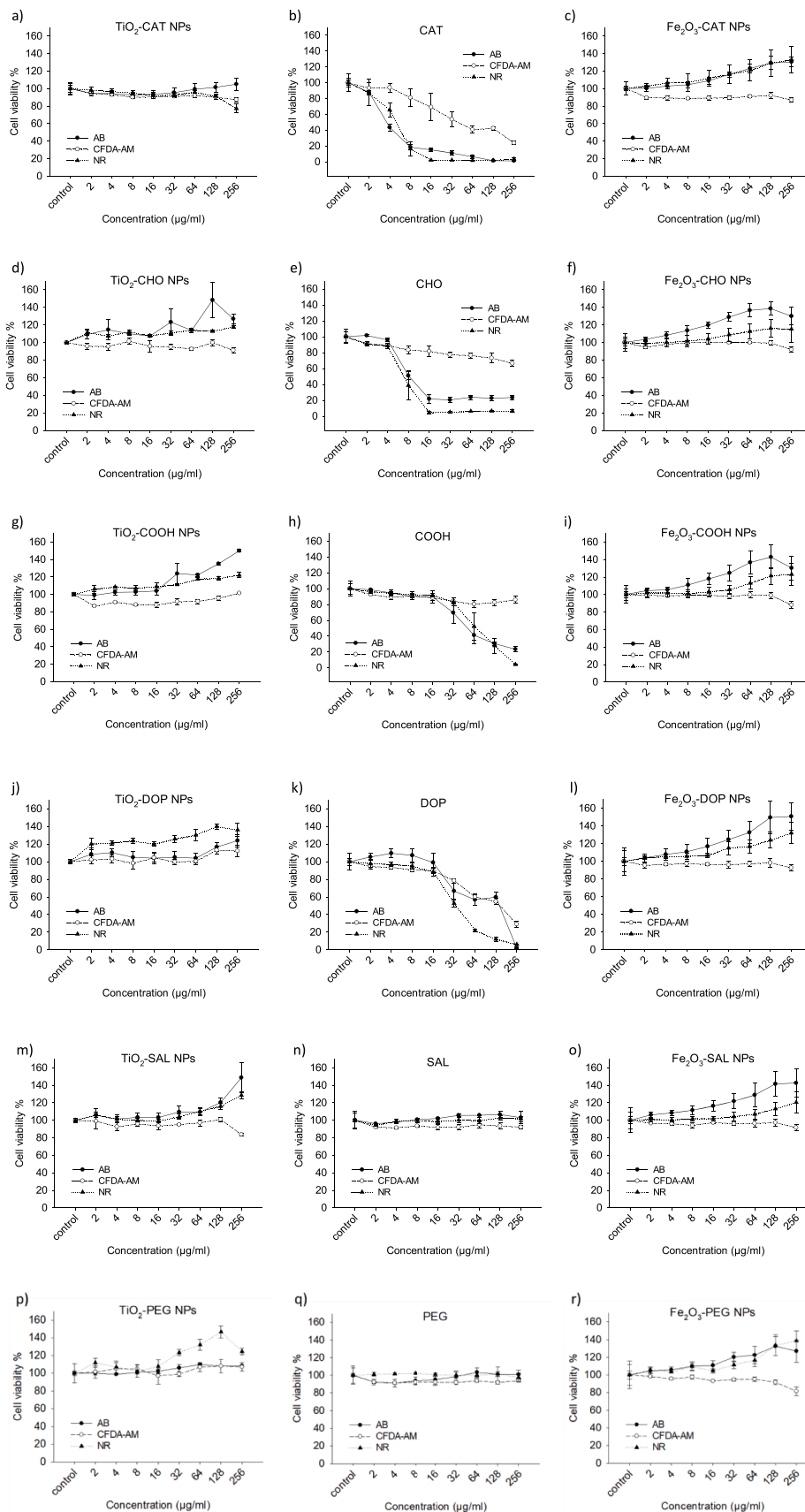
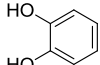
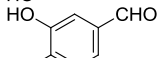
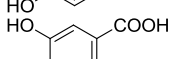
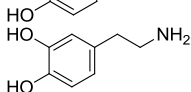


Fig. 3. Dose-response curves for modified  $\text{TiO}_2$  NPs (a, d, g, j, m, p), organic ligands only (b, e, h, k, n, q), and modified  $\text{Fe}_2\text{O}_3$  NPs (c, f, i, l, o, r) as measured by the three cytotoxicity assays (AB, CFDA-AM, and NR). Values represent the mean  $\pm$  standard error of the mean (n = 3).

**Table 2**

EC<sub>50</sub> values (95% Confidence Interval) for catechol molecules considering the three cytotoxicity assays (AB, CFDA-AM, and NR).

	Ligand	AB ( $\mu\text{g}\cdot\text{mL}^{-1}$ )	CFDA-AM ( $\mu\text{g}\cdot\text{mL}^{-1}$ )	NR ( $\mu\text{g}\cdot\text{mL}^{-1}$ )
CAT		4.0 (3.8 – 5.3)	53 (37 – 86)	4.8 (4.4 – 5.4)
CHO		9.5 (6.5 – 15)	-	7.0 (6.3 – 8.2)
COOH		61 (42 – 85)	-	70 (55 – 78)
DOP		91 (73 – 129)	120 (100 – 135)	36 (33 – 41)

toxicity, with significant effects at  $32 \mu\text{g}\cdot\text{mL}^{-1}$  and EC<sub>50</sub> values higher by about one order of magnitude. For CAT and CHO, cell viability dropped sharply, reaching levels below 20% compared to the control at 8 and  $16 \mu\text{g}\cdot\text{mL}^{-1}$ , respectively, while COOH produced such inhibitory effects only at the highest tested concentration ( $256 \mu\text{g}\cdot\text{mL}^{-1}$ ). Unlike the other catechols, DOP showed a different behaviour for the NR and AB assays in the descending portion of the dose-response curve, and consequently rather different EC<sub>50</sub> values, but in both testing systems it caused a complete loss of cell viability at the highest tested concentration.

As already mentioned, plasma membrane integrity, as measured by the CFDA-AM assay, seemed to be less affected by the examined compounds, except for DOP. CAT elicited significant effects at already  $8 \mu\text{g}\cdot\text{mL}^{-1}$  but then showed a slower decrease in cell viability compared to the AB and NR assays (Fig. 3). Similarly, CHO seemed to cause only a slight impairment of plasma membrane integrity, while COOH did not show significant effects even at the highest tested concentration. For the CFDA-AM assay, therefore, EC<sub>50</sub>s could be calculated only for CAT and DOP. The different response obtained with this assay, already observed for other toxicants (Dayeh et al., 2013), could indicate that these ligands may impair cell metabolism and lysosomal functions, but have a lower or no impact on plasma membrane integrity, suggesting the existence of specific mechanisms of toxic action (Schweigert et al., 2001).

The comparison of our findings with those from other *in vitro* cytotoxicity assays is unavoidably affected by a limited availability of literature data (Table S3). Anyhow, it can be seen that the result for SAL, which showed no cytotoxicity in PLHC-1 cells up to the tested concentrations ( $256 \mu\text{g}\cdot\text{mL}^{-1}$ ), is in accordance with previous studies that observed EC<sub>50</sub> values greater than  $500 \mu\text{g}\cdot\text{mL}^{-1}$  in a variety of cell lines, or even in the same cell line with a different endpoint assay (Caminada et al. 2006). Moreover, the order of toxicity exhibited by the four catechol compounds is similar to that observed for rat hepatocytes, except for dopamine; PLHC-1 cells seemed also to show a higher sensitivity, but this could be ascribed to the significantly lower exposure time in rat hepatocytes.

Though no single study examined the whole set of ligands and very few data are available for CHO, DOP and PEG, our results show in general a good agreement with studies on acute toxicity to aquatic organisms, both in terms of sensitivity and of relative toxicity of the different compounds (Table S3). Only for SAL some organisms seemed to exhibit a higher sensitivity, but acute toxicity values for this compound vary considerably among different studies, and some authors suggest a possible overestimation of toxicity due to the low pH of the testing solutions (Pino et al., 2016; Henschel et al., 1997) (Table S3).

As far as the modified NPs are concerned, no reduction in cell viability was observed (Fig. 3), except for a slight decrease - but statistically significant (metadata file, SI) - observed in the CFDA-AM assay for TiO<sub>2</sub>-COOH NPs in the range from 2 to  $64 \mu\text{g}\cdot\text{mL}^{-1}$ , and for TiO<sub>2</sub>-

CAT, TiO<sub>2</sub>-SAL, Fe<sub>2</sub>O<sub>3</sub>-PEG NPs only at the highest concentration tested ( $256 \mu\text{g}\cdot\text{mL}^{-1}$ ). The low decrease in cell viability shown by TiO<sub>2</sub>-COOH NPs could be ascribed to the fact that the carboxylic groups of COOH molecules may partly be involved in their grafting on the NPs' surface (Korpany et al., 2017), leading to a surface coating whose interactions with cellular structures probably affect the membrane integrity.

These findings show that, once the catecholate ligands get covalently attached to the surface of TiO<sub>2</sub> and Fe<sub>2</sub>O<sub>3</sub> NPs, they do not seem to exert the same toxic effect on PHLC-1 cells, observed for these chemicals already at  $\sim 4 \mu\text{g}\cdot\text{mL}^{-1}$ . However, since the same exposure concentrations ( $4$ - $256 \mu\text{g}\cdot\text{mL}^{-1}$ ) were used in all assays, it has to be taken into account that the ligands' actual concentration was lower in the tests with modified NPs than in those with free ligands, depending on the amount attached on NPs. Thus, to compare the concentrations of free ligands that exerted toxic effects with the corresponding concentrations of modified NPs, a conversion was carried out for TiO<sub>2</sub>-CAT NPs, based on percent coverage as estimated from the results of TGA analysis (providing total mass loss %). As a result, the inhibition of metabolic activity and lysosomal functioning caused by CAT at  $4 \mu\text{g}\cdot\text{mL}^{-1}$  should occur at a concentration of  $102 \mu\text{g}\cdot\text{mL}^{-1}$  for TiO<sub>2</sub>-CAT NPs and  $160 \mu\text{g}\cdot\text{mL}^{-1}$  for Fe<sub>2</sub>O<sub>3</sub>-CAT NPs, since the measured mass losses were 3.9% and 2.5% for TiO<sub>2</sub>-CAT and Fe<sub>2</sub>O<sub>3</sub>-CAT NPs respectively (see Table 1). However, at these concentrations modified NPs did not show a decrease of cell viability, suggesting that the cytotoxic action of catechol is inhibited when this compound is attached to the nanoparticle surface.

To confirm that the absence of modified NPs cytotoxicity was not due to the low ligand concentration on the surface of the NPs, we increased the surface coverage of TiO<sub>2</sub> and Fe<sub>2</sub>O<sub>3</sub> NPs by using different grafting procedures. Catechol was selected for these experiments because it exerted toxic effects already at  $4 \mu\text{g}\cdot\text{mL}^{-1}$ . The tested conditions included i) increase of the organic ligand concentration, ii) heating of the dispersion at increasing temperatures, and iii) heating in the solid state (Table S4, together with the organic percent mass loss determined by TGA). As can be seen, the reaction performed without solvent, by heating the NP powder with the solid ligand up to the melting point of the catechol, and then by heating the mixture at  $80^\circ\text{C}$  for 1 hour (Entry 3, Table S4), led to the highest mass coverage (8.5% for TiO<sub>2</sub>-CAT NPs, compared to 3.9% obtained under conventional conditions). Thus, the same conditions were used to increase the coverage of Fe<sub>2</sub>O<sub>3</sub> NPs (Entry 6, Table S4), leading to a coverage of 4.4%, almost double than the 2.5% obtained under the conventional conditions. As already observed for the ligand grafting performed at room temperature in ethanol (Table 1), the increase in the coverage mass was smaller than that observed for TiO<sub>2</sub> NPs.

Moreover, to verify that no morphological modifications occurred after the grafting of the ligands, pristine and TiO<sub>2</sub> NPs modified with catechol (obtained both under the conventional conditions and by heating at  $80^\circ\text{C}$  in the solid state) were analysed by SEM. As reported in Fig. 4, the size ( $38 \pm 15 \text{ nm}$ ) and shape of both coated NPs was similar (Fig. 3c-f), and unchanged with respect to the pristine material (Fig. 3a, b). In addition, as expected for metal oxide NPs, aggregates with sizes ranging from 200 nm up to the micron were observed, suggesting that the grafting of the organic ligands is limited by the formation of such macrostructures and probably occurs only on the surface of these agglomerates.

The modified NPs with increased coverage (called TiO<sub>2</sub>-CAT NPs-3 and Fe<sub>2</sub>O<sub>3</sub>-CAT NPs-1) were both tested to verify if the absence of cytotoxicity previously observed could be ascribed to a low degree of coverage. Both TiO<sub>2</sub> CAT NPs-3 and Fe<sub>2</sub>O<sub>3</sub>-CAT NPs-1 still showed no decrease in cell viability up to the highest concentration tested ( $256 \mu\text{g}\cdot\text{mL}^{-1}$ ) (Fig. 5), and the dose-response curves were similar to those previously obtained with a lower coverage (Fig. 2). Therefore, the increased level of coverage did not induce a corresponding increase of cytotoxic effects.

Based on these findings, we may infer that the grafting on TiO<sub>2</sub> and Fe<sub>2</sub>O<sub>3</sub> NPs played a role in inhibiting the toxicity of the examined

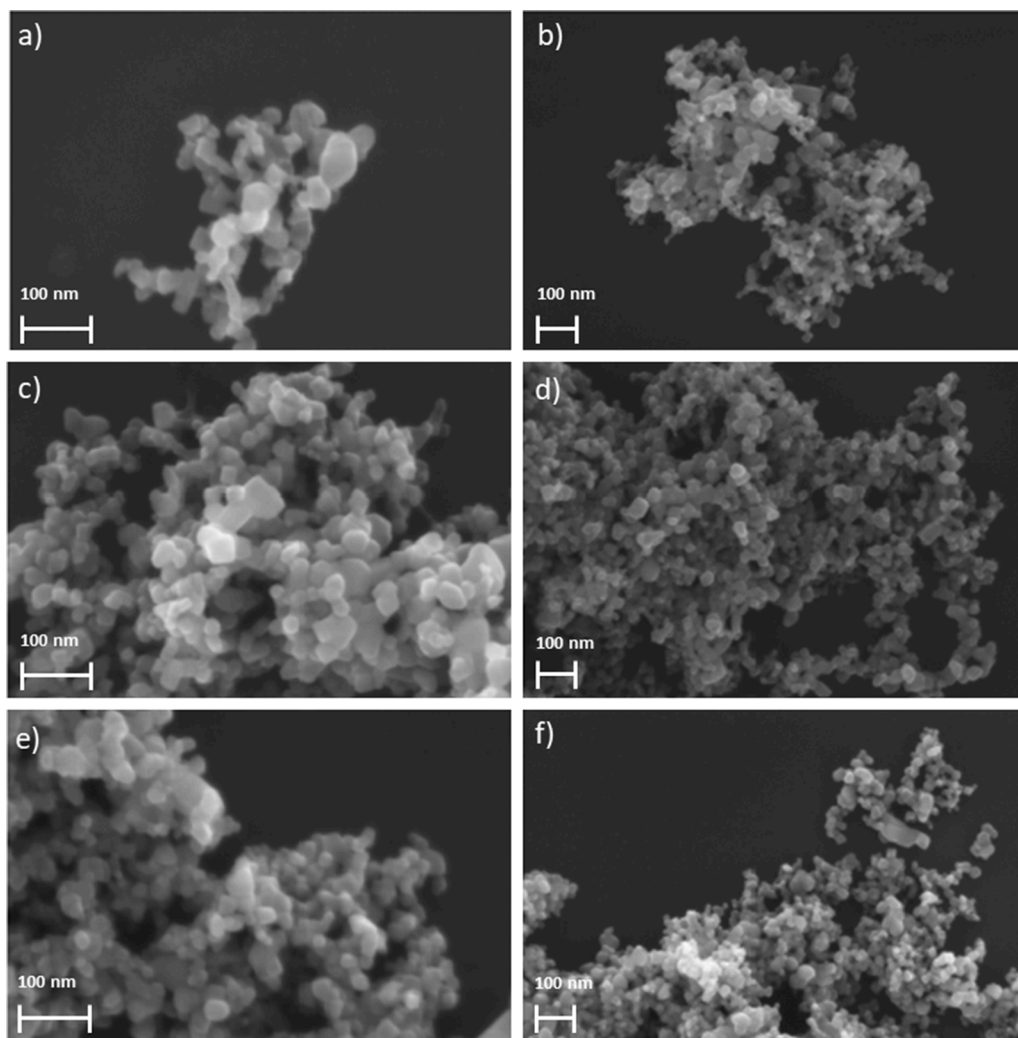


Fig. 4. SEM images of (a, b) pristine  $\text{TiO}_2$  NPs, (c, d)  $\text{TiO}_2$ -CAT NPs obtained in EtOH at room temperature, (e, f)  $\text{TiO}_2$ -CAT NPs-3 obtained in the solid state at  $80^\circ\text{C}$ .

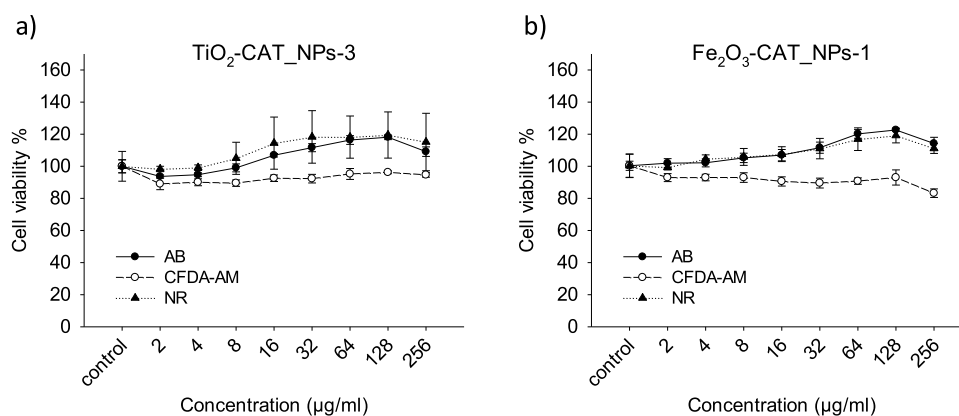


Fig. 5. Dose-response curves for surface-modified  $\text{TiO}_2$  (a) and  $\text{Fe}_2\text{O}_3$  (b) NPs with increased organic coating as measured by the three cytotoxicity assays (AB, CFDA-AM, and NR) in PLHC-1 cell line. Values represent the mean  $\pm$  standard error of the mean ( $n=3$ ).

catechol compounds. Since the hydroxyl groups are known to be involved in the toxic action of this type of molecules, though different mechanisms may contribute (Schweigert et al., 2001), the overall results of this study suggest that the toxicity exerted by the catechol type ligands is lost once their -OH groups bind to the surface of the tested NPs.

#### 4. Conclusions

Catechol and catecholate-ligands bearing different functional moieties (i.e., carboxylate, aldehyde and amine groups), together with SAL and PEG polymer, were selected to investigate the interaction of organic molecules with metal oxide nanoparticles and how their attachment on the NPs' surface may affect their possible toxic action. Despite the



significant cytotoxicity observed for the catechol type ligands, none of the modified NPs tested caused a similar cytotoxic effect in the topminnow fish hepatoma cell line (PLHC-1), even after increasing the percentage of the grafted organic molecules by means of different ways of synthesis. These results indicate that an inhibition of catechols cytotoxicity is achieved by the grafting to TiO<sub>2</sub> or Fe<sub>2</sub>O<sub>3</sub> NPs, which exerted no toxic effects in the bare state. This behaviour may be ascribed to the complexation of the two -OH groups of catechols with Ti and Fe at the NPs' surface. Since grafting could occur spontaneously in the environment, these findings suggest that TiO<sub>2</sub> and Fe<sub>2</sub>O<sub>3</sub> NPs could act as sorbents of catechol-like pollutants potentially present in surface waters, reducing their toxicity and detrimental effects, though the long-term stability of these interactions is still poorly known. Lastly, the good agreement found between *in vitro* cytotoxicity determined with the PLHC-1 cell line and acute *in vivo* toxicity for catechols suggests that the application of multiple cell viability assays based on different endpoints is a valuable alternative to *in vivo* assays, in compliance with principle of the 3Rs (Replacement, Reduction and Refinement).

### CRedit authorship contribution statement

**Elena Badetti:** Conceptualization, Data curation, Formal analysis, Investigation, Methodology, Project administration, Supervision, Writing – original draft, Writing – review & editing. **Andrea Brunelli:** Conceptualization, Data curation, Formal analysis, Investigation, Methodology, Writing – original draft, Writing – review & editing. **Eleonora Faraggiana:** Data curation, Writing – original draft, Writing – review & editing. **Judit Kalman:** Data curation, Formal analysis, Investigation, Methodology, Writing – original draft, Writing – review & editing. **Cinzia Bettiol:** Investigation, Validation, Writing – review & editing. **Francesca Caterina Izzo:** Formal analysis, Investigation, Writing – review & editing. **José Maria Navas:** Conceptualization, Funding acquisition, Methodology, Project administration, Resources, Validation, Writing – review & editing. **Antonio Marcomini:** Conceptualization, Funding acquisition, Resources, Validation, Writing – review & editing.

### Declaration of Competing Interest

The authors declare that they have no known competing financial interests or personal relationships that could have appeared to influence the work reported in this paper

### Data Availability

Data is available in the Supporting Information

### Acknowledgments

The authors are grateful to the European Commission for funding SUN project (FP7-NMP-2013-LARGE-7, Grant Agreement N° 604305) and NanoFASE project (H2020-NMP-28-2014, Grant Agreement N° 646002).

### Supplementary materials

Supplementary material associated with this article can be found, in the online version, at doi:10.1016/j.aquatox.2022.106291.

### References

Ali, A., Zafar, H., Zia, M.U.I., Haq, I., Phull, A.R., Ali, J.S., Hussain, A., 2016. Synthesis, characterization, applications, and challenges of iron oxide nanoparticles. *Nanotechnol. Sci. Appl.* 9, 49–67. <https://doi.org/10.2147/NSA.S99986>.

- Alkilany, A.M., Lohse, S.E., Murphy, C.J., 2013. The gold standard: gold nanoparticle libraries to understand the nano-bio interface. *Acc. Chem. Res.* 46, 650–661. <https://doi.org/10.1021/ar300015b>.
- Badetti, E., Calgaro, L., Falchi, L., Bonetto, A., Bettiol, C., Leonetti, B., Ambrosi, E., Zendri, E., Marcomini, A., 2019. Interaction between copper oxide nanoparticles and amino acids: influence on the antibacterial activity. *Nanomaterials* 9. <https://doi.org/10.3390/nano9050792>.
- Barreto, G., Madureira, D., Capani, F., Aon-Bertolino, L., Saraceno, E., Alvarez-Giraldez, L.D., 2009. The role of catechols and free radicals in benzene toxicity: an oxidative DNA damage pathway. *Environ. Mol. Mutagen.* 50, 771–780. <https://doi.org/10.1002/em.20500>.
- Basti, H., Ben Tahar, L., Smiri, L.S., Herbst, F., Vaulay, M.-J., Chau, F., Ammar, S., Benderbous, S., 2010. Catechol derivatives-coated Fe<sub>3</sub>O<sub>4</sub> and γ-Fe<sub>2</sub>O<sub>3</sub> nanoparticles as potential MRI contrast agents. *J. Colloid Interface Sci.* 341, 248–254. <https://doi.org/10.1016/j.jcis.2009.09.043>.
- Bermejo-Nogales, A., Connolly, M., Rosenkranz, P., Fernández-Cruz, M.-L., Navas, J.M., 2017. Negligible cytotoxicity induced by different titanium dioxide nanoparticles in fish cell lines. *Ecotoxicol. Environ. Saf.* 138, 309–319. <https://doi.org/10.1016/j.ecoenv.2016.12.039>.
- Brunelli, A., Badetti, E., Basei, G., Izzo, F.C., Hristozov, D., Marcomini, A., 2018. Effects of organic modifiers on the colloidal stability of TiO<sub>2</sub> nanoparticles. A methodological approach for NPs categorization by multivariate statistical analysis. *NanoImpact* 9, 114–123. <https://doi.org/10.1016/j.impact.2018.03.001>.
- Castano, A., Gómez-Lechón, M.J., 2005. Comparison of basal cytotoxicity data between mammalian and fish cell lines: a literature survey. *Toxicol. Vitro* 19, 695–705. <https://doi.org/10.1016/j.tiv.2005.04.002>.
- Dayeh, V.R., Bols, N.C., Tanneberger, K., Schirmer, K., Lee, L.E.J., 2013. The use of fish-derived cell lines for investigation of environmental contaminants: an update following OECD's fish toxicity testing framework No. 171. *Curr. Protoc. Toxicol.* 56 <https://doi.org/10.1002/0471140856.tx0105s56>, 1.5.1-1.5.20.
- Fernández-Cruz, M.L., Lammel, T., Connolly, M., Conde, E., Barrado, A.I., Derick, S., Perez, Y., Fernandez, M., Furger, C., Navas, J.M., 2013. Comparative cytotoxicity induced by bulk and nanoparticulated ZnO in the fish and human hepatoma cell lines PLHC-1 and Hep G2. *Nanotoxicology* 7, 935–952. <https://doi.org/10.3109/17435390.2012.676098>.
- Fiege, H., Voges, H.-W., Hamamoto, T., Umemura, S., Iwata, T., Miki, H., Fujita, Y., Buysch, H.-J., Garbe, D., Paulus, W., 2000. Phenol derivatives. *Ullmann's Encyclopedia of Industrial Chemistry*. American Cancer Society. [https://doi.org/10.1002/14356007.a19\\_313](https://doi.org/10.1002/14356007.a19_313).
- Gaiser, B.K., Fernandes, T.F., Jepson, M., Lead, J.R., Tyler, C.R., Stone, V., 2009. Assessing exposure, uptake and toxicity of silver and cerium dioxide nanoparticles from contaminated environments. *Environmental Health: A Global Access Science Source*. <https://doi.org/10.1186/1476-069X-8-S1-S2>.
- Galbis-Martínez, L., Fernández-Cruz, M.L., Alte, L., Valdehita, A., Rucandio, I., Navas, J.M., 2018. Development of a new tool for the long term *in vitro* ecotoxicity testing of nanomaterials using a rainbow-trout cell line (RTL-W1). *Toxicol. Vitro* 50, 305–317. <https://doi.org/10.1016/j.tiv.2018.04.007>.
- Henschel, K.P., Wenzel, A., Diedrich, M., Fliedner, A., 1997. Environmental hazard assessment of pharmaceuticals. *Regul. Toxicol. Pharmacol.* 25, 220–225. <https://doi.org/10.1006/rtp.1997.1102>.
- Jensen, K.A., Kembouche, Y., Christiansen, E., Jacobsen, N., Wallin, H., Guiot, C., Spalla, O., Witschger, O., 2011. The generic NANOGENOTOX dispersion protocol: final protocol for producing suitable manufactured nanomaterial exposure media.
- Kalman, J., Merino, C., Fernández-Cruz, M.L., Navas, J.M., 2019. Usefulness of fish cell lines for the initial characterization of toxicity and cellular fate of graphene-related materials (carbon nanofibers and graphene oxide). *Chemosphere* 218, 347–358. <https://doi.org/10.1016/j.chemosphere.2018.11.130>.
- Korpany, K.V., Majewski, D.D., Chiu, C.T., Cross, S.N., Blum, A.S., 2017. Iron oxide surface chemistry: effect of chemical structure on binding in benzoic acid and catechol derivatives. *Langmuir* 33, 3000–3013. <https://doi.org/10.1021/acs.langmuir.6b03491>.
- Lai, X., Wei, Y., Zhao, H., Chen, S., Bu, X., Lu, F., Qu, D., Yao, L., Zheng, J., Zhang, J., 2015. The effect of Fe<sub>2</sub>O<sub>3</sub> and ZnO nanoparticles on cytotoxicity and glucose metabolism in lung epithelial cells. *J. Appl. Toxicol.* 35, 651–664. <https://doi.org/10.1002/jat.3128>.
- Lammel, T., Boisseaux, P., Fernández-Cruz, M.-L., Navas, J.M., 2013. Internalization and cytotoxicity of graphene oxide and carboxyl graphene nanoplatelets in the human hepatocellular carcinoma cell line Hep G2. *Part. Fibre Toxicol.* 10, 27. <https://doi.org/10.1186/1743-8977-10-27>.
- Lammel, T., Navas, J.M., 2014. Graphene nanoplatelets spontaneously translocate into the cytosol and physically interact with cellular organelles in the fish cell line PLHC-1. *Aquat. Toxicol.* 150, 55–65. <https://doi.org/10.1016/j.aquatox.2014.02.016>.
- Lammel, T., Sturve, J., 2018. Assessment of titanium dioxide nanoparticle toxicity in the rainbow trout (*Onchorynchus mykiss*) liver and gill cell lines RTL-W1 and RTgill-W1 under particular consideration of nanoparticle stability and interference with fluorometric assays. *NanoImpact* 11, 1–19. <https://doi.org/10.1016/j.impact.2018.01.001>.
- Lynch, I., Weiss, C., Valsami-Jones, E., 2014. A strategy for grouping of nanomaterials based on key physico-chemical descriptors as a basis for safer-by-design NMs. *Nano Today* 9, 266–270. <https://doi.org/10.1016/j.nantod.2014.05.001>.
- Nel, A., Xia, T., Meng, H., Wang, X., Lin, S., Ji, Z., Zhang, H., 2013. Nanomaterial toxicity testing in the 21st century: use of a predictive toxicological approach and high-throughput screening. *Acc. Chem. Res.* 46, 607–621. <https://doi.org/10.1021/ar300022h>.

- Piccinno, F., Gottschalk, F., Seeger, S., Nowack, B., 2012. Industrial production quantities and uses of ten engineered nanomaterials in Europe and the world. *J. Nanoparticle Res.* 14, 1109. <https://doi.org/10.1007/s11051-012-1109-9>.
- Pino, M.R., Muniz, S., Val, J., Navarro, E., 2016. Phytotoxicity of 15 common pharmaceuticals on the germination of *Lactuca sativa* and photosynthesis of *Chlamydomonas reinhardtii*. *Environ Sci Pollut Res* 23, 22530–22541.
- Rajiv, S., Jerobin, J., Saranya, V., Nainawat, M., Sharma, A., Makwana, P., Gayathri, C., Bharath, L., Singh, M., Kumar, M., Mukherjee, A., Chandrasekaran, N., 2016. Comparative cytotoxicity and genotoxicity of cobalt (II, III) oxide, iron (III) oxide, silicon dioxide, and aluminum oxide nanoparticles on human lymphocytes in vitro. *Hum. Exp. Toxicol.* 35 (2), 170–183. <https://doi.org/10.1177/0960327115579208>.
- Reeves, J.F., Davies, S.J., Dodd, N.J.F., Jha, A.N., 2008. Hydroxyl radicals ( $\cdot\text{OH}$ ) are associated with titanium dioxide ( $\text{TiO}_2$ ) nanoparticle-induced cytotoxicity and oxidative DNA damage in fish cells. *Mutat. Res.* 640, 113–122. <https://doi.org/10.1016/j.mrfmmm.2007.12.010>.
- Savić, T.D., Comor, M.I., Nedeljković, J.M., Veljković, D., Zarić, S.D., Rakić, V.M., Janković, I.A., 2014. The effect of substituents on the surface modification of anatase nanoparticles with catecholate-type ligands: a combined DFT and experimental study. *Phys. Chem. Chem. Phys.* 16, 20796–20805. <https://doi.org/10.1039/c4cp02197e>.
- Schweigert, N., Zehnder, A.J.B., Eggen, R.I.L., 2001. Chemical properties of catechols and their molecular modes of toxic action in cells, from microorganisms to mammals. *Environ. Microbiol.* 3, 81–91. <https://doi.org/10.1046/j.1462-2920.2001.00176.x>.
- Shang, L., Nienhaus, K., Nienhaus, G.U., 2014. Engineered nanoparticles interacting with cells: size matters. *J. Nanobiotechnology.* <https://doi.org/10.1186/1477-3155-12-5>.
- Slomberg, D.L., Ollivier, P., Miche, H., Angeletti, B., Bruchet, A., Philibert, M., Brant, J., Labille, J., 2019. Nanoparticle stability in lake water shaped by natural organic matter properties and presence of particulate matter. *Sci. Total Environ.* 656, 338–346. <https://doi.org/10.1016/j.scitotenv.2018.11.279>.
- Subramanyam, R., Mishra, I.M., 2008. Treatment of catechol bearing wastewater in an upflow anaerobic sludge blanket (UASB) reactor: sludge characteristics. *Bioresour. Technol.* 99, 8917–8925. <https://doi.org/10.1016/j.biortech.2008.04.067>.
- Sun, T., Zhang, Y.S., Pang, B., Hyun, D.C., Yang, M., Xia, Y., 2014. Engineered nanoparticles for drug delivery in cancer therapy. *Angew. Chemie Int. Ed.* 53, 12320–12364. <https://doi.org/10.1002/anie.201403036>.
- Yuen, A.K.L., Hutton, G.A., Masters, A.F., Maschmeyer, T., 2012. The interplay of catechol ligands with nanoparticulate iron oxides. *Dalt. Trans.* 41, 2545–2559. <https://doi.org/10.1039/C2DT11864E>.
- Zhao, L., Lv, B., Yuan, H., Zhou, Z., Xiao, D., 2007. A sensitive chemiluminescence method for determination of hydroquinone and catechol. *Sensors.* <https://doi.org/10.3390/s7040578>.